Response evaluation and vibration control of a transmission tower-line system in mountain areas subjected to cable rupture

Bo Chen, Jingbo Wu, Yiqin Ouyang[*] and Deng Yang

Hubei Key Laboratory of Roadway Bridge & Structural Engineering, Wuhan University of Technology, Wuhan 430070, China

Abstract.   Transmission tower-line systems are commonly slender and generally possess a small stiffness and low structural damping. They are prone to impulsive excitations induced by cable rupture and may experience strong vibration. Excessive deformation and vibration of a transmission tower-line system subjected to cable rupture may induce a local destruction and even failure event. A little work has yet been carried out to evaluate the performance of transmission tower-line systems in mountain areas subjected to cable rupture. In addition, the control for cable rupture induced vibration of a transmission tower-line system has not been systematically conducted. In this regard, the dynamic response analysis of a transmission tower-line system in mountain areas subjected to cable rupture is conducted. Furthermore, the feasibility of using viscous fluid dampers to suppress the cable rupture-induced vibration is also investigated. The three dimensional (3D) finite element (FE) model of a transmission tower-line system is first established and the mathematical model of a mountain is developed to describe the equivalent scale and configuration of a mountain. The model of a tower-line-mountain system is developed by taking a real transmission tower-line system constructed in China as an example. The mechanical model for the dynamic interaction between the ground and transmission lines is proposed and the mechanical model of a viscous fluid damper is also presented. The equations of motion of the transmission tower-line system subjected to cable rupture without/with viscous fluid dampers are established. The field measurement is carried out to verify the analytical FE model and determine the damping ratios of the example transmission tower-line system. The dynamic analysis of the tower-line system is carried out to investigate structural performance under cable rupture and the validity of the proposed control approach based on viscous fluid dampers is examined. The made observations demonstrate that cable rupture may induce strong structural vibration and the implementation of viscous fluid dampers with optimal parameters can effectively suppress structural responses.

Keywords: transmission tower-line system; cable rupture; response control; viscous fluid damper; contact force; field measurement

1. Introduction

Nowadays, transmission tower-line systems are widely built throughout the world to provide electricity supply services. However, often exposed in the open air, transmission lines are

---

∗Corresponding author, E-mail: cemqdwhut@163.com

inevitably subjected to corrosion-induced damage. Engineering metal material can be converted to more stable mineral compounds when exposed to corrosive environments for certain periods (Chen and Xu 2005). The corrosion action can change the chemical and physical properties of metal material and weaken the strength of transmission lines. The degradation of metal material due to corrosion effects is of importance for the durability of the transmission line as a whole and may lead to damage accumulation and cable rupture eventually. If transmission lines are subjected to strong external loads associated with accumulating damages induced by corrosive environments, structural safety will be threatened and the damage may finally cause cable rupture, resulting in huge economic losses. Several transmission line accidents that caused extensive structural damage occurred in recent years in Canada, France and China, not described in the open literature, suggesting that efforts should be directed to a better understanding of the behavior of transmission line structures under dynamic loads (Kaminski *et al.* 2008). To be a typical type of high-rise steel structures, transmission tower-line systems are commonly slender and generally possess small stiffness and low structural damping (Li *et al.* 2005, Chen *et al.* 2014). Thus, they are prone to impulsive excitations induced by cable rupture and may experience oscillations. The design codes of transmission tower-line systems of many countries suggest that the loads and structural performance due to cable rupture should be assessed (ASCE 1991, 2000; IEC 2003).

To understand the performance of transmission tower-line systems subjected to cable rupture, many theoretical, experimental and field measurement investigations have been carried out during the past two decades. Irvine (1981) systematically investigated cable vibration through theoretical deduction. Then, with the rapid development of numerical simulation techniques, a transmission line can be modelled by using various cable elements and analyzed by using nonlinear FE methods. Kaminski *et al.* (2008) investigated the model uncertainty in the assessment of transmission line towers subjected to cable rupture. The dynamic response of transmission line towers subjected to cable rupture was predicted by the use of various models with different degrees of sophistication or detailing. To suppress the vibration due to cable rupture, a transmission tower-line system needs some measures to abate their dynamic responses (Housner *et al.* 1997, Spencer and Nagarajaiah 2003). To increase structural stiffness is traditionally an effective approach while it is often uneconomical (Balendra *et al.* 2001, Li *et al.* 2015, Chen *et al.* 2015). Many dynamic absorbers have been proposed to suppress excessive structural vibrations such as tuned liquid damper and tuned mass damper (Soong and Dargush 1997, Parulekar and Reddy 2009). Dynamic absorbers can effectively reduce dynamic responses of flexible tower structures while they often need a place to be installed and this requirement may conflict with structural function and usage (Hitchcock *et al.* 1999, Ghorbani-Tanha *et al.* 2009). Therefore, various energy dissipating devices, such as viscous fluid dampers, have been developed recently as an alternative approach for dynamic mitigation of flexible truss towers.

A little work has yet been carried out to evaluate the performance of transmission tower-line systems in mountain areas subjected to cable rupture. In addition, the control for cable rupture induced vibration of a transmission tower-line system has not been systematically conducted. In this regard, the dynamic response analysis of a transmission tower-line system in mountain areas subjected to cable rupture is conducted. Furthermore, the feasibility of using viscous fluid dampers to suppress cable rupture-induced vibration is also actively investigated in this study. The three dimensional (3D) FE model of a transmission tower-line system is first established and transmission lines are modeled by using cable elements. The mathematical model of a mountain is developed to describe the equivalent scale and configuration of the mountain. The model of a tower-line-mountain system is developed by taking a real transmission tower-line system

constructed in China as an example. The mechanical model for the dynamic interaction between the ground and transmission lines is proposed and the mechanical model of a viscous fluid damper is also presented. The equations of motion of the transmission tower-line system subjected to cable rupture without/with viscous fluid dampers are established. The field measurement is carried out to verify the analytical FE model and determine the damping ratios of the example transmission tower-line system. The dynamic analysis of the tower-line system is conducted to investigate the structural performance under cable rupture and the validity of the proposed control approach based on viscous fluid dampers is examined. The made observations demonstrate that cable rupture may induce strong structural vibration and the implementation of viscous fluid dampers with optimal parameters can suppress dynamic responses effectively in particular for peak velocity and acceleration.

2. Model of transmission tower-line system in mountain areas

2.1 Model of transmission tower-line system

To be a typical spatial structure, a transmission tower can be constructed by using truss members based on finite element (FE) methods. The mass matrix M_t and the stiffness matrix K_t of a transmission tower in the global coordinate system (GCS) can be expressed as follows

$$\mathbf{M}_t = \sum_{i=1}^{ne} \mathbf{T}^{(i)T} \mathbf{M}^{(i)} \mathbf{T}^{(i)} \tag{1}$$

$$\mathbf{K}_t = \sum_{i=1}^{ne} \mathbf{T}^{(i)T} \mathbf{K}^{(i)} \mathbf{T}^{(i)} \tag{2}$$

where *ne* is the number of elements of the tower model; $M^{(i)}$ denotes the element mass matrix of the *i*th element in the GCS; $K^{(i)}$ denotes the element mass matrix of the *i*th element in the GCS; $T^{(i)}$ is the freedom transform matrix from the local coordinate system (LCS) to the GCS. A transmission line can be modeled by using cable elements to take nonlinear effects into consideration. The stiffness matrix of the *i*th cable element $\mathbf{K}_c^{(i)}$ of a transmission line in the GCS can be expressed as the sum of the elastic stiffness matrix $\mathbf{K}_e^{(i)}$ and the stress stiffness matrix $\mathbf{K}_\sigma^{(i)}$.

$$\mathbf{K}_c^{(i)} = \mathbf{K}_e^{(i)} + \mathbf{K}_\sigma^{(i)} \tag{3}$$

The elastic stiffness matrix $\mathbf{K}_e^{(i)}$ can be constructed by using structural strain

$$\mathbf{K}_e^{(i)} = \mathbf{T}_i^T \cdot \overline{\mathbf{K}}_e^{(i)} \cdot \mathbf{T}_i \tag{4}$$

where $\overline{\mathbf{K}}_e^{(i)}$ denotes the stiffness matrix of the ith cable element in a transmission line in the LCS; T_i denotes the transformation matrix for the degrees of freedom of the ith cable element.

The stress stiffness matrix $\mathbf{K}_\sigma^{(i)}$ is constructed by using the element stress and shape function

of a cable element.

$$\mathbf{K}_\sigma^{(i)} = \frac{N_i}{L_i} \begin{bmatrix} 1 & & & & & \\ 0 & 1 & & & sym & \\ 0 & 0 & 1 & & & \\ -1 & 0 & 0 & 1 & & \\ 0 & -1 & 0 & 0 & 1 & \\ 0 & 0 & -1 & 0 & 0 & 1 \end{bmatrix} \tag{5}$$

where N_i is the axial force of the ith cable element; L_i is the length of the ith cable element.

The global stiffness matrix of a transmission line K_l can be determined by combining all the element stiffness matrices in the GCS. The mass matrix of a transmission line M_l in the GCS can be written by using a lumped mass matrix or a consistent mass matrix. The global stiffness and mass matrices of a transmission tower-line system in the GCS can be established by combining the stiffness and mass matrices of towers and lines in the GCS

$$\mathbf{K} = \mathbf{K}_t + \sum_{j=1}^{nl} \mathbf{K}_l^{(j)} \tag{6}$$

$$\mathbf{M} = \mathbf{M}_t + \sum_{j=1}^{nl} \mathbf{M}_l^{(j)} \tag{7}$$

where *nl* is the numbers of transmission lines in a tower-line system.

2.2 Model of mountain

It is well-known that many transmission tower-line systems are constructed in mountain areas. Transmission lines inevitably fall down on mountain surfaces when subjected to cable rupture. It is necessary to take the contact effects between transmission lines and mountains into consideration. Thus, the analytical models of mountains, supporting transmission tower-line systems, required to be established. One approach is to develop a mathematical model to describe the equivalent scale and configuration of the mountain. By simplifying geometric shapes of typical mountains, a two dimensional model of a mountain can be expressed as

$$z = \frac{R^2}{R^2 + x^2} H \tag{8}$$

where: H denotes the height of the mountain; R denotes the equivalent radius of the mountain base; x denotes the horizontal coordinates of mountain nodes; z denotes of the vertical coordinates of mountain nodes. The 3D mountain models can be developed by expanding the 2D models into the 3D space

$$z = \frac{R^2}{R^2 + x^2 + y^2} H \tag{9}$$

where: *x* and *y* denote the horizontal coordinates of the mountain node in the x and y directions, respectively.

2.3 Model of transmission tower-line-mountain system

The analytical model of a transmission tower-line system in mountain areas can be established by combine the model of tower-line system as well as the model of mountains. A real transmission tower-line system constructed in southern coastal mountain areas of China as shown in Fig. 1 is taken as an example to illustrate the configuration of the tower-line-mountain coupling model.
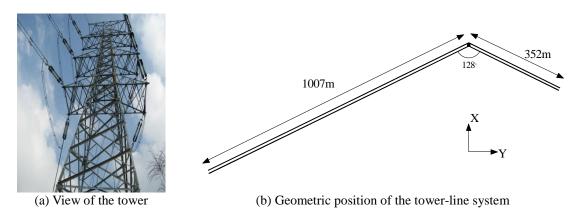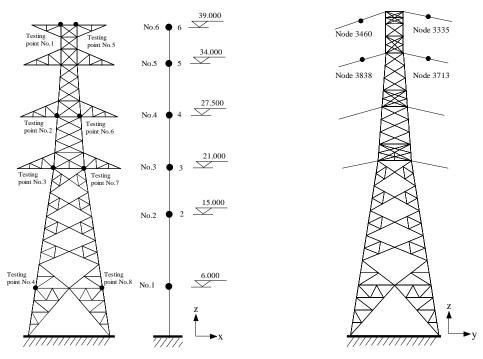

(a) View of the tower   (b) Geometric position of the tower-line system

Fig. 1 View of the transmission tower-line system

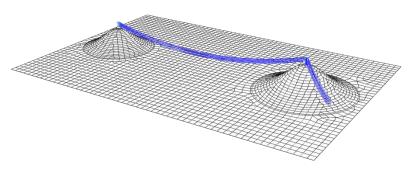Fig. 2 Configuration and six nodal floors of the transmission tower

Fig. 3 Analytical model of the tower-line-mountain system

Fig. 2 shows the configuration of the example transmission tower. The elevation of the tower is 39m and the distance between two tower bases is 10.1 m. The structural members used in the transmission tower are made of Q235 steel with a yielding stress of 235 MPa. The Young's modulus of steel metal is 2.01×10^{11} N/m^2 and the density is 7800 kg/m^3. Vertical major members, skew members, cross arms and platforms of the tower are formed as a spatial truss tower. Five platforms are connected to vertical major members to form cross arms and tower body and skew members are incorporated to increase the vertical and lateral stiffness of the whole tower. Four cross arms are constructed in the upper parts of the tower body for the connection of transmission lines. Two ground wires located on the top cross arm of the tower and the other six transmission lines are installed on the other three cross arms. The insulator lengths of ground wires and overhead transmission lines are 0.5 m and 4.5 m respectively. The tower and its two adjacent towers are located on top of three small hills. The long span and short span of the transmission tower are 1007 m and 352 m, respectively. The angle between two spans is about 128 degrees. The height of the mountain supporting the transmission tower is 164.1 m and the height of the adjacent mountain in the long span is 138.7 m. The model of the transmission tower-line-mountain system is displayed in Fig. 3.

3. Equation of motion of transmission tower-line system

3.1 Contact effects between the ground and transmission lines

Owing to the application of various numerical techniques, the researches on contact mechanics have been improved substantially to study the contact body with complicated geometric configuration and material properties. The solution systems and approaches based on numerical computation have been established gradually in recent years. In the contact analysis of a tower-line-mountain system, the contact areas between transmission lines and the ground are generally not known in advance. In addition the finite element models of contacting bodies are generated is such a way that precise node-to-node contact is neither achievable nor desirable when contact is established. This type of contact situation precludes the use of node-to-node contact elements has the capability to represent general contact of models that are generated with arbitrary meshes. Contact kinematics is concerned with the precise tracking of contact nodes and surfaces in order to define clear and unambiguous contact conditions. Commonly, the penalty method of satisfying contact compatibility is available for the contact analysis on a transmission tower-line-mountain system. The contact force can be expressed as:

$$f_n = \begin{cases} K_n d & \text{if } d \le 0 \\ 0 & \text{if } d > 0 \end{cases} \tag{10}$$

where K_n denotes the contact stiffness between the ground and the falling transmission lines; d denotes the magnitude of the gap.

Tangential forces are due to friction that arises as the contact node of the falling transmission lines meets and moves along the ground. The contact effects can be considered based on three friction models: frictionless, elastic Coulomb friction, and rigid Coulomb friction. The Coulomb friction representation requires the specification of the coefficient of sliding friction μ. For the frictionless case the tangential force is merely:

$$f_x = f_y = 0 \tag{11}$$

For elastic Coulomb friction, it is necessary to calculate the tangential deformations of the contact node relative to the target. Location of the contact nodes in the falling transmission lines on the ground shows the total motion of contact node along the target plane. It is seen that the total tangential displacement is represented by the projection of the total contact node motion to the unwarped plane of the target.

3.2 Equation of motion of a transmission tower-line system

Fluids can also be used to dissipate energy and numerous device configurations and materials have been proposed. Viscous fluid dampers are proposed to realize the energy dissipation for civil engineering structures under dynamic excitations by utilizing the mechanism of viscous effects. There is a considerable progress in developing varieties of viscous fluid devices for structural vibration control since the 1980s. (Constantinou *et al.* 1993). The viscous nature of the device is obtained through the use of specially configured orifices so as to generate damper forces. A viscous fluid damper generally consists of a piston in the damper housing filled with a compound of silicone or oil and it can dissipate energy through movement of the piston in the highly viscous fluid. If the fluid is purely viscous (for instance, Newtonian), then the output force of the damper is directly proportional to the velocity of the piston. Over a large frequency range, the damper exhibits viscoelastic fluid behavior, which can be commonly described by the Maxwell model. The damping force of a viscous fluid damper can be expressed as

$$P(t) = C_0 \, \text{sgn}[\dot{x}(t)] |\dot{x}(t)|^\alpha \tag{12}$$

where: α denotes the velocity exponent of the viscous damper; C_0 denotes the viscous coefficient; sgn[ ] denotes the symbol function.

The equation of motion of a transmission tower-line system, in terms of the relative displacement vector $\mathbf{x}(t)$ with respect to its base is written by (Xu and Qu 2003)

$$\mathbf{M}\ddot{\mathbf{x}}(t) + \mathbf{C}\dot{\mathbf{x}}(t) + \mathbf{K}\mathbf{x}(t) = \mathbf{W}(t) + \mathbf{F}(t) \tag{13}$$

where: $\ddot{\mathbf{x}}(t)$, $\dot{\mathbf{x}}(t)$ and $\mathbf{x}(t)$ are the displacement, velocity and acceleration responses, respectively; $\mathbf{M}$, $\mathbf{C}$ and $\mathbf{K}$ are mass, damping and stiffness matrices of the tower-line system, respectively; $\mathbf{W}(t)$

is the impulsive excitation induced by cable rupture; $\mathbf{F}(t)$ is and the contact force vector.

The Rayleigh damping assumption is adopted to construct the structural damping matrix and the damping ratios in the first two modes of vibration are set based on field measurement. The equations of motion of the structure-damper system can be expressed as follows (Xu and Qu 2003)

$$\mathbf{M\ddot{x}}(t) + \mathbf{C\dot{x}}(t) + \mathbf{Kx}(t) = \mathbf{W}(t) + \mathbf{F}(t) + \mathbf{Hu}(t) \tag{14}$$

$$\mathbf{F}(t) = \left[\mathbf{F}_n(t), \mathbf{F}_x(t), \mathbf{F}_y(t) \right] \tag{15}$$

where: $\mathbf{H}$ is the loading influence matrix reflecting the location of viscous fluid dampers; $\mathbf{u}(t)$ is the control force vector of viscous fluid dampers; n is the total number of viscous fluid dampers in the system. $\mathbf{F}_n(t)$ is the vertical contact force vector; $\mathbf{F}_x(t)$ and $\mathbf{F}_y(t)$ are the tangential contact force vectors in the local x and y direction, respectively; $\mathbf{u}(t)$ is the control force vector of dampers.

4. System identification of the transmission tower-line system

The modal testing and identification methods based on ambient excitation (Yi *et al.* 2011, 2013, Lei *et al.* 2012) may be an alternative approach for system identification to be performed. The field measurement and system identification of the tower-line system are carried out in this study. The dynamic responses of the example tower subjected to ambient excitations are collected through field measurement and utilized to identify the dynamic properties and damping ratios by using the Natural Excitation Technique (NExT) with the Eigensystem Realization Algorithm (ERA) and the Stochastic Subspace Identification (SSI) techniques. The dynamic responses of the tower are collected by using the portable vibration testing system INV and the accelerometer 941-B made in China. Two sampling frequencies, 30 Hz and 100 Hz, are selected and the testing duration for each sample is 300s. The identified dynamic properties of the transmission tower by using the two approaches are listed in Table 1.

Table 1 Dynamic properties of the transmission tower (Hz)

No.	Freq.	f_1	f_2	f_3	f_4	f_5
1	Coupled tower (FEM)	3.481	3.541	6.678	7.755	7.929
2	Coupled tower (NExT+ERA)	3.292	3.312	6.129	7.116	7.382
	Error (1 and 2)	**5.429%**	**6.467%**	**8.221%**	**8.241%**	**6.899%**
3	Coupled tower (SSI)	3.322	3.292	6.209	7.183	7.411
	Error (1 and 3)	**4.568%**	**7.032%**	**7.023%**	**7.376%**	**6.533%**
	Damping ratio (NExT+ERA)	1.842%	2.113%	2.191%	1.782%	2.443%
	Damping ratio (SSI)	2.132%	1.891%	1.971%	2.132%	2.243%

The results of different testing sets are averaged as the identified natural frequencies and damping ratios. The made observations indicate that the peak acceleration responses at different testing points are different to a great extent, but the spectrum properties of all the points are quite similar. The identified natural frequencies of the two approaches are quite close while the errors by the SSI are slightly smaller than those by the NExT+ERA. It is also seen that the damping ratios of the first two mode shapes are about 2%, which is used to construct the Rayleigh damping matrix in the subsequent numerical simulation.

5. Dynamic responses of tower-line system under cable rupture

5.1 Falling process of transmission lines

The dynamic responses of the example transmission tower-line system in mountain areas subjected to cable rupture are analyzed in this section. Four cases of cable rupture are considered to investigate the effects of rupture location on the dynamic responses of the transmission tower and lines, respectively. The detailed information of rupture cases is listed in Table 2 and displayed in Fig. 4.

The whole process of the cable rupture of the example transmission tower-line system is computed and displayed in Fig. 5 for case 1. The analytical results demonstrate that when the rupture event occurs at the left end of the shield wire, an obvious impulsive excitation is produced in the transmission tower-line system to induce the strong vibration of the coupled system. Then, the broken shield wire is quickly falling down due to the gravity force of the wire. Parts of the broken shield wires fall on the mountain surface shortly after 5.3s and a strong collision between the wire and mountain is observed, which may induce the quick fluctuation in the dynamic responses and internal forces of the transmission lines and wires. The dynamic interaction between the broken wire and the ground may exist for certain durations and then the vibration may decay gradually. The vibration duration of the whole process of the cable rupture is about 30s for the example transmission tower-line system. The falling simulation of the other three cases is also carried out and the corresponding 3D results are similar to that of case 1 and not displayed here due to page limitation. The dynamic responses of insulators, tower and transmission lines are demonstrated and discussed in the following sections.

Table 2 Cases of cable rupture of transmission lines

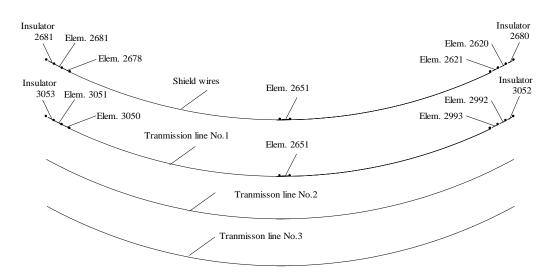| No.	Span	Location	Element No.
Case 1	Long span	Left end, Shield wire	2679
Case 2	Long span	Right end, Shield wire	2620
Case 3	Long span	Left end, Line 1	3051
Case 4	Long span	Right end, Line 1	2992

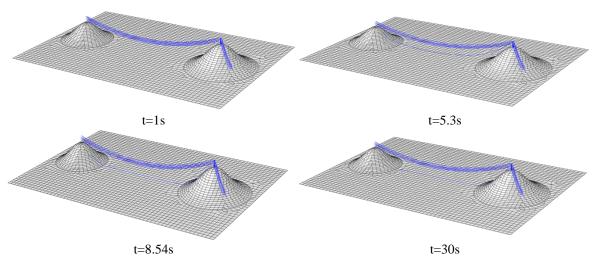Fig. 4 Position of nodes and elements of transmission lines

Fig. 5 The falling process of the transmission lines under cable rupture

5.2 Responses of insulators

The location of typical insulators is depicted in Fig. 2. The displacement responses of insulators in the long span are investigated and displayed in Fig. 6.

It is seen that the cable rupture may induce strong vibrations of transmission lines in both the x and y directions. The curves in Fig. 6 indicate that the cable rupture in the shield wire (cases 1 and 2) may cause strong vibrations in connecting insulator (node 3460) while the dynamic responses of other insulators (node 3838) in adjacent transmission line 1 are quite small. To compare cases 1 and 2, one can find that the displacement responses of node 3460 induced by the cable rupture at the right end of the shield wire are much larger than those at the left end. This observation

indicates that the vibrations induced by cable rupture present distinct properties of localization and may decay quickly along the broken transmission line. In addition, it is found that the cable rupture in the long span may cause a quick increase in the insulator displacement in the short span while the following vibration fluctuations are very small in comparison with those in the long span. This is because the cable rupture in the long span induces strong unbalance forces to the transmission tower-line system and cause the deformation of the tower and lines. This observation indicates that the impulsive effects of cable rupture in the current span are much larger than those in the adjacent span.

5.3 Responses of transmission tower

The displacement responses of the transmission tower with cable rupture are computed and displayed in Fig. 7 and the peak displacement at the top of the tower are listed in Table 2. The curves in Fig. 7 clearly indicate that the cable rupture cause strong impulsive excitation to the transmission tower and obvious response spikes occur shortly after the rupture associated with the following response fluctuations. Then, the vibration decays gradually and the displacement approaches to a constant magnitude, which is actually the static deformation caused by the rupture-induced unbalance forces. The data in Table 3 demonstrate that the effects of cable rupture in the shield wire on the tower displacement are slightly larger than those in transmission line 1. This is because the rupture-induced impulsive excitation in the shield wire (cases 1 and 2) is acting on top of the tower, whose loading position is slightly higher than that in transmission line 1 (cases 3 and 4). In addition, the peak displacement responses in the x direction are much larger than those in the y direction. This is because the included angles between transmission lines and the x direction is much larger than the counterparts between transmission lines and the y direction, which may lead to a larger decomposed component of the rupture-induced impulsive excitation in the x direction. To compare the displacement time histories of the tower and insulators shown in Figs. 6 to 7, one can easily find that the peak responses and vibration fluctuation of the insulators in the long span is much larger than those in the tower. Furthermore, the peak responses and vibration fluctuation of the insulators in the adjacent span is substantially smaller than those in the long span and the tower. This observation further indicates that the impulsive effects induced by the cable rupture present the properties of localization and quick reduction.
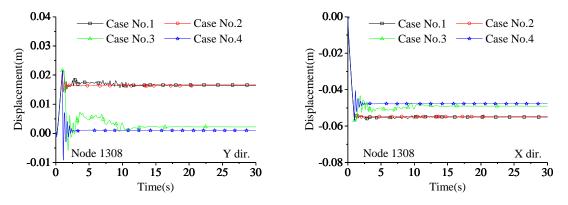

Fig. 7 Displacement responses on top of the tower

Table 3 Comparison of peak displacement at the top of tower

	Direction	Case 1	Case 2	Case 3	Case 4
With contact	X dir. (mm)	56.32	55.64	52.42	49.56
With contact	Y dir. (mm)	18.96	17.82	7.37	7.18
Without contact	X dir. (mm)	56.32	55.64	52.42	49.56
Without contact	Y dir. (mm)	18.96	17.82	7.37	7.18

5.4 Responses of transmission lines

The effects of cable rupture on the internal forces of transmission lines are also analyzed and the corresponding axial stresses are displayed in Figs. 8 and 9, respectively, for the shield wire and transmission line 1.
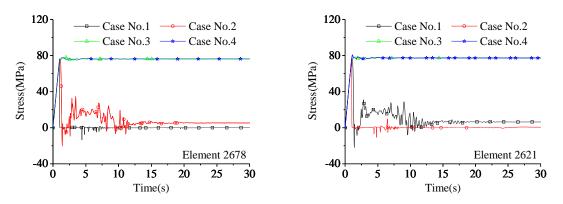

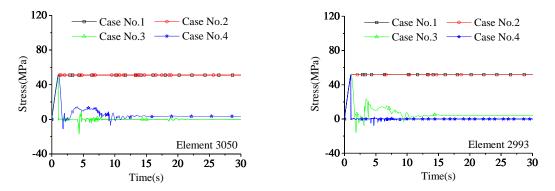Fig. 8 Element stress of the shield wire

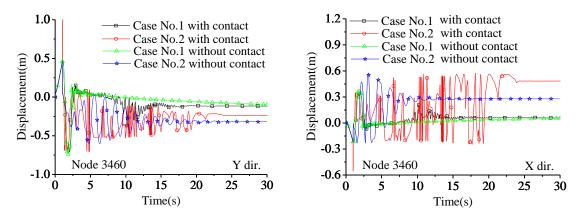Fig. 9 Element stress of transmission line 1

Fig. 10 Comparison of dynamic responses with and without contact

It is seen from Fig. 8 that if the rupture event occurs in the shield wire (cases 1 or 2), there may exist a very strong spike in stress time histories and then the stress may fluctuate first and then decay to a constant value gradually. In case 1, element 2678 is adjacent to fractured element 2679 and its stress is finally close to zero because the looseness of cable force due to the cable rupture. Similarly, element 2621 is on the other side of the shield wire and apart from fractured element 2679 and its final stress is a certain value which is the gravity of the fractured line. The stresses of the two elements in line 1, namely elements 3050 and 2993, are about 50 MPa and no obvious fluctuations can be observed due to the rapid decay of rupture impulse. It is also seen that the final stress of element 3050 is almost the same as that of element 2993.

5.5 Effects of gruond contact

The dynamic responses of the tower-line system with and without contact are compared as shown in Fig. 10. It is seen that the displacement responses with contact effects present much more fluctuations than those without contact effects due to the dynamic impact of the falling lines to the ground. Similar observations can be made from the time histories of velocity and acceleration responses. The wire stresses without contact increase quickly and the magnitudes are much larger than those with contact. Clearly, the observations of the wire stress without contact are unreasonable because the wire may fall down to the ground very shortly and the stresses are induced by the wire gravity, which are actually are constant values. Therefore, it is essential to consider the contact effects in the dynamic simulation of the transmission tower-line system because it can accurately describe the dynamic interactions of the transmission lines with the ground.

6. Response control of the tower-line system under cable rupture

6.1 Comparison on damper installation schemes

It is known that the parameters of viscous fluid dampers should be set in advance and cannot be

changed during actual structural vibration. Three kinds of exponent parameter α of viscous fluid dampers, 0.2, 0.3, and 0.4, are selected respectively for vibration control. Sixteen viscous fluid dampers are designed to be installed in the transmission tower to suppress the structural vibration induced by cable rupture. Four installation schemes of viscous fluid dampers are considered to investigate the effects of damper position on control efficacy as shown in Fig. 11. For scheme 1, all the dampers are incorporated into the vertical major members in the upper part of the tower. For scheme 2, all the dampers are incorporated in the members of four cross arms. For scheme 3, all the dampers are incorporated into the skew members in the upper part of the tower. For scheme 4, all the dampers are incorporated into the vertical major members in the lower part of the tower.

The maximum responses of the transmission tower in the two horizontal directions without/with viscous fluid dampers are computed and compared as shown in Fig. 12. The exponent parameters α for all the damper installation schemes are set at 0.3. It is observed that the implementation of viscous fluid dampers can substantially reduce the peak velocity of the transmission tower. The satisfactory control performance can be achieved if the damping coefficient c is reached by 350 kN.s/mm. To increase the damping coefficient c can increase the damper control force, but cannot remarkably improve the control performance. Similar observations can be made from the results of the peak acceleration and displacement. It is also seen that the control performance of peak acceleration is quite similar to those of the peak velocity, while the control efficacy of peak displacement is inferior to that of the peak velocity and acceleration. The possible reason is that the impulse induced by the cable rupture may cause strong initial velocity and acceleration in the tower-line system while the induced initial displacement is small. Therefore, the magnitudes of structural displacement responses are relatively small in comparison with those of velocity and acceleration responses, which are quite different from structural dynamic responses under strong winds or earthquakes.

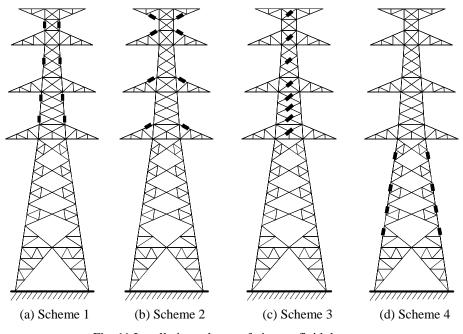(a) Scheme 1   (b) Scheme 2   (c) Scheme 3   (d) Scheme 4

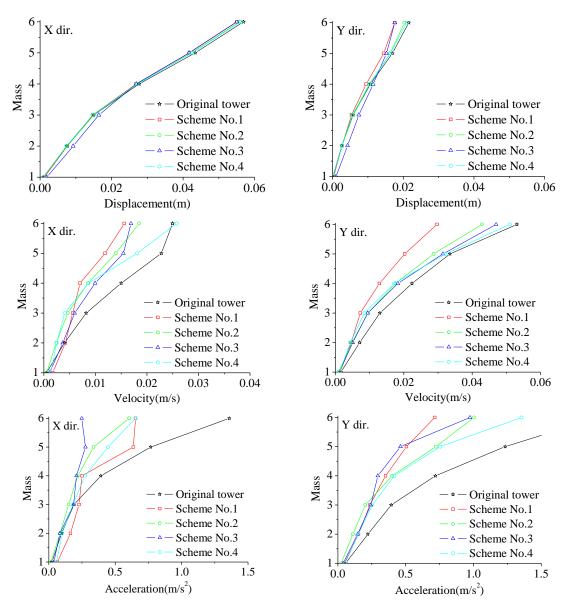Fig. 11 Installation scheme of viscous fluid dampers

Fig. 12 Comparison on control performance of different schemes

The observations in Fig. 12 demonstrate that the entire control performance of schemes 1 and 2 is slightly better than that of schemes 3 and 4. Thus, it can be understood that the optimal positions for the dampers are located in the vertical major and skew members in the upper parts of the tower. Further investigation indicates that the control performance for the peak acceleration of scheme 3 is slightly better than that of scheme 1 while the control efficacy for the peak velocity is opposite. In reality, the damper installation in the skew members is much easier than that in the vertical major members in real application. Therefore, the damper installation scheme 3 is adopted for the parametric study in the following sections.

6.2 Effects of exponent parameter

As mentioned before, the parameter of viscous fluid dampers should be set in advance and cannot be changed during real structural vibration. The control force produced by the damper is tightly related to the velocity exponent α. and the increase in exponent parameter actually leads to the increase of damper force. Therefore, the effects of damper force on control efficacy are examined in this section through changing velocity exponent.
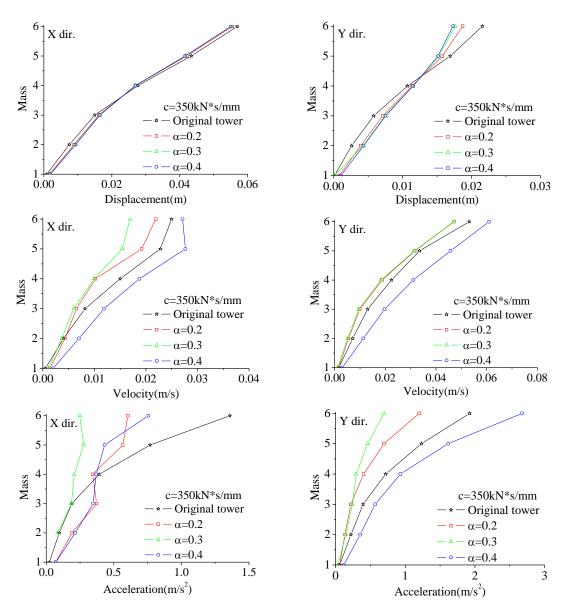

Fig. 13 Comparison on control performance with different exponent parameters

The peak responses of the transmission tower without/with viscous fluid dampers are computed and compared as shown in Fig. 13. It is observed that the incorporation of viscous dampers into the tower can reduce the peak displacement of the transmission tower. The satisfactory control performance of the vibration in the x direction can be achieved if the velocity exponent is set at 0.3. In addition, it is found that to further increase the velocity exponent cannot remarkably improve the control performance. Nevertheless, the control performance of peak velocity in the y direction is slightly inferior to that in the x direction for all the three exponent parameters. The control performance of the peak acceleration is similar to that of the peak velocity, while the control efficacy of the peak displacement is inferior to that of the peak velocity and acceleration.
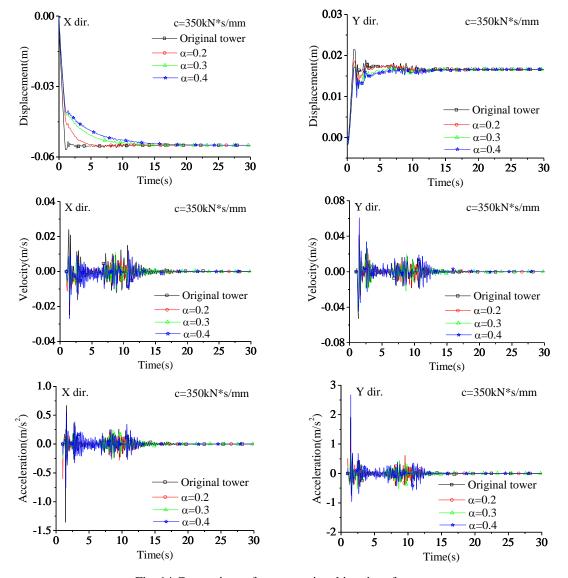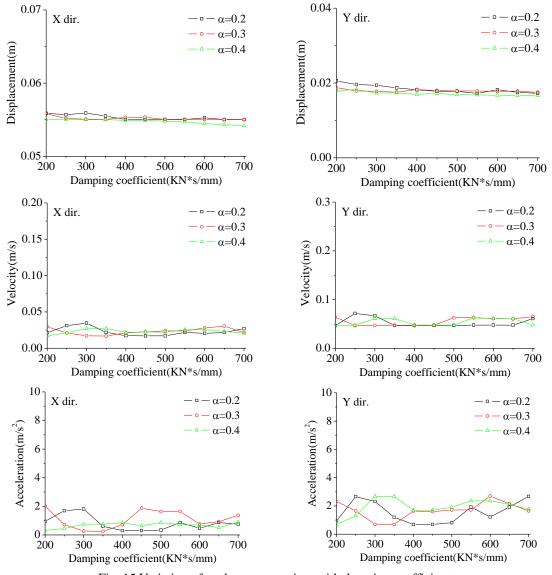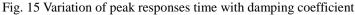

Fig. 14 Comparison of response time histories of tower

Fig. 15 Variation of peak responses time with damping coefficient

Demonstrated in Fig. 14 are the displacement, velocity and acceleration time histories on top of the tower without/with viscous fluid dampers. The comparison between the four sets of time histories clearly reveals that the viscous fluid dampers can be used to mitigate the structural dynamic responses induced by the cable rupture. The control performance of velocity and acceleration responses is much better than that of acceleration responses. To compare the damper performance with different velocity exponents, one can find that the increase of exponent parameters can gradually improve the control performance. The control efficacy with α=0.3 is much better than that with α=0.2, in particular for the velocity and acceleration responses.

However, when the velocity exponent reaches above 0.3, a further increase of the exponent parameter will not have any further significant response reduction. Therefore, the optimal exponent parameter for the control of the example tower-line system is set at 0.3.

6.3 Effects of damping coefficient

The variations of the peak responses on top of the tower with damping coefficients are analyzed and displayed in Fig. 15. The exponent parameter for the control of the example tower-line system is set at 0.3. It is seen that almost all the three types of the dynamic responses of the tower can be reduced when the damping coefficient increases from 200 to 700 kN.s/mm. The curves in Fig. 15 indicate that the peak displacement gradually decreases with increasing damping coefficients. No matter which nodal floor is considered, there is an optimal value of damping coefficient by which the satisfactory performance of the viscous fluid damper can be achieved. If the control forces of viscous fluid dampers increase after reaching the optimal values, the damper performance cannot be improved substantially and tends to remain the same. A possible explanation of such a phenomenon is that at the optimal value of a viscous fluid damper, the damper can slip as much as possible under the given excitation intensity and the damper can best dissipate the structural vibration energy. If the control force increases from the optimal value, the energy dissipation capacity of the damper cannot be improved remarkably because a large control force may frustrate the damper slippage during vibration. The variations of the peak velocity present similar characteristics compared to the peak displacement, while the control performance of the peak acceleration fluctuates to a slight extent. It is not beneficial to set a very large damping coefficient for viscous fluid dampers so as to avoid unnecessary cost waste. The optimum damping coefficient for the control of the example transmission tower-line system is about 350 kN.s/mm.

7. Conclusions

The feasibility of using viscous fluid dampers to suppress the vibration of a transmission tower-line system subjected to cable rupture actively investigated in this study. The mathematical model of a mountain is developed and the model of the tower-line-mountain system is developed by taking a real transmission tower-line system as an example. The mechanical model for the dynamic interaction between the ground and transmission lines is proposed. The equations of motion of the transmission tower-line system subjected to cable rupture without/with viscous fluid dampers are established for response evaluation and vibration control. The field measurement is carried out to verify the analytical FE model and determine the damping ratios of the example transmission tower-line system. The validity of the proposed control approach based on viscous fluid dampers is examined through a parametric study in detail.

The made observations demonstrate that the impulsive effects induced by cable rupture present the properties of localization and quick reduction and the impulsive effects of cable rupture in the current span are much larger than those in the adjacent span. The viscous fluid damper can be used in the vibration control of the transmission tower-line system with cable rupture because of its simple configuration as well as satisfactory energy-dissipating capacity. The control performance of velocity and acceleration responses is much better than that of displacement responses and the control efficacy of schemes 1 and 3 is better than that of schemes 2 and 4. There exist optimal values of the velocity exponent by which the satisfactory control performance can be achieved and the control efficacy cannot

be improved substantially and almost keep stable after reaching the optimal values. The parametric study reveals that there exists an optimum damping coefficient of a viscous fluid damper for the response control and an increment in the damping coefficient cannot remarkably improve the control performance and leads to the unnecessary cost consumption.

Acknowledgments

References

ASCE-American Society of Civil Engineers (1991), *Guideline for electrical transmission line structural loading*, ASCE Manuals and Reports on Engineering Practice, No. 74, New York.

ASCE-American Society of Civil Engineers (2000), *ASCE Standard 10-97: Design of latticed steel transmission structures*, 2000, New York.

Balendra, T., Wang, C.M. and Yan. N. (2001), "Control of wind-excited towers by active tuned liquid column damper", *Eng. Struct.*, **23**(4), 1054-1067.

Chen, B., Guo, W.H., Li, P.Y. and Xie. W.P. (2014), "Dynamic responses and vibration control of the transmission tower-line system: a state-of-the-art-review", *The Scientific World Journal*, Article ID **538457**, 1-20.

Chen, B., Xiao, X., Li, P.Y. and Zhong. W. L. (2015), "Performance evaluation on transmission-tower line system with passive friction dampers subjected to wind excitations", *Shock Vib.*, Article ID **310458**, 1-13.

Chen, B., Xu, Y.L. and Qu, W.L. (2005), "Evaluation of atmospheric corrosion damage to steel space structures in coastal areas", *Int. J. Solids Struct.*, **42**(16-17), 4673-4694.

Constantinou, M.C., Symans, M.D., Tsopelas, P. and Taylor, D.P. (1993), "Fluid viscous dampers in applications of seismic energy dissipation and seismic isolation", *Proc. of ATC J7-J Seminar on Seismic Isolation, Passive Energy Dissipation, and Active Control*, **2**, 581-592.

Ghorbani-Tanha, A.K., Noorzad, A. and Rahimian. M. (2009), "Mitigation of wind-induced motion of Milad Tower by tuned mass damper", *Struct. Des.Tall Spec.Build.*, **18**(4), 371-385.

Hitchcock, P.A. et al. (1999), "Damping properties and wind-induced response of a steel frame tower fitted with liquid column vibration absorbers", *J. Wind Eng. Ind. Aerod.*, **83**(1-3), 183-196.

Housner, G.W., Bergman, L.A., Caughey, T.K., Chassiakos, A.G., Claus, R.O., Masri, S.F., Skelton, R.E., Soong, T.T., Spencer, Jr B.F. and Yao, T.P. (1997), "Structural control: Past, present, and future", *J. Eng. Mech. - ASCE*, **123**(9), 897-971.

IEC-International Electrotechnical Commission (2003), *IEC 60826: Design criteria of overhead transmission lines*.

Irvine, H.M. (1981), *Cable structure*, The MIT, Press, New York.

Kaminski., Jr. J., Riera, J.D. and De Menezes, R.C.R. (2008), "Model uncertainty in the assessment of transmission line towers subjected to cable rupture", *Eng. Struct.*, **30**(10), 2935-2944.

Lei, Y., Jiang Y.Q. and Xu Z.Q.(2012), "Structural damage detection with limited input and output measurement signals", *Mech. Syst. Signal Pr.*, **28**, 229-243.

Li, H.N., Shi, W.L., Wang, G.X. and Jia LG (2005), "Simplified models and experimental verification for coupled transmission tower-line system to seismic excitations", *J. Sound Vib.*, **286**(3), 569-585.

Li, L., Song, G., Singla M. and Mo Y.L. (2015), "Vibration control of a traffic signal pole using a pounding tuned mass damper with viscoelastic materials (II): experimental verification", *J. Vib. Control*, **21**(4),

670-675.

Parulekar, Y.M. and Reddy, G.R. (2009), "Passive response control systems for seismic response reduction: a state-of-the-art review", *Int. J. Struct. Stab. Dynam.*, **9**(1), 151-177.

Soong, T.T. and Dargush, G.F. (1997), *Passive energy dissipation systems in structural engineering*, Wiley, Chichester, U.K.

Spencer, B.F. Jr. and Nagarajaiah, S. (2003), "State of the art of structural control", *J. Struct. Eng. - ASCE*, **129**(7), 845-856.

Xu, Y.L. and Qu. W. L. (2003), "Active/robust moment controllers for seismic response control of a large span building on top of ship lift towers", *J. Sound Vib.*, **261**(2), 277-296.

Yi, T.H., Li, H.N and Gu, M. (2013), "Wavelet based multi-step filtering method for bridge health monitoring using GPS and accelerometer", *Smart Struct. Syst.*, **11**(4), 331-348.

Yi, T.H., Li, H.N and Gu, M. (2011), "Optimal sensor placement for structural health monitoring based on multiple optimization strategies", *Struct. Des. Tall Spec. Build.*, **20** (7), 881-900.